



## Preparation of Nickel Oxide Microparticles by Pulsed Laser Ablation and Application to Gas Sensors

Nedal A. Hussain <sup>a\*</sup>, Luma Y. Abbas <sup>b</sup>, Lamyaa A. Latif <sup>c</sup>

<sup>a</sup> Department of Physics, College of Science, Mustansiriyah University, Baghdad, Iraq.

[nedalali44@uomustansiriyah.edu.iq](mailto:nedalali44@uomustansiriyah.edu.iq)

<sup>b</sup> Department of Physics, College of Science, Mustansiriyah University, Baghdad, Iraq.

[lumaphysics2203@uomustansiriyah.edu.iq](mailto:lumaphysics2203@uomustansiriyah.edu.iq)

<sup>c</sup> Department of Physics, College of Science, Mustansiriyah University, Baghdad, Iraq.

[lamyaa1967@uomustansiriyah.edu.iq](mailto:lamyaa1967@uomustansiriyah.edu.iq)

\*Corresponding author.

Submitted: 07/02/2020

Accepted: 10/04/2021

Published: 25/06/2021

### KEY WORDS

Nickel Oxide, Pulsed laser ablation, Gas Sensing Semiconductor

### ABSTRACT

*Nickel oxide (NiO) microparticles were synthesized by pulsed laser ablation in double deionized water and intensively studied using Nd:YAG laser. The obtained sample was examined by X-ray diffraction, XRD measurement which tests the existence of polycrystalline. The structural parameters introduced and surface morphology was studied using field emission scanning electron microscopy devices. The optical properties of microparticles in a liquid were investigated through UV-VIS spectroscopy. The CO/CO<sub>2</sub> sensing properties of the NiO microstructure sensors were systematically investigated, and the effects of different laser fluencies on the CO/CO<sub>2</sub> sensing characteristics were analyzed. XRD measurements reflected the existence of polycrystalline, the optical result shows that The absorption spectra peak centered around 360 nm and a tail extending to the red region (600 nm), the scanning electron microscopy images showed that the morphologies of NiO thin films have microspheres in various. The sample affected by laser fluence 1.9 J/cm<sup>2</sup> which exhibits the best sensitivity for CO<sub>2</sub> gas.*

**How to cite this article:** N. A. Hussain, L.Y. Abbas and L. A. Latif , "Preparation of nickel oxide microparticles by pulsed laser ablation and application to gas Sensors," Engineering and Technology Journal, Vol. 39, No. 06, pp. 1011-1018, 2021.

DOI: <https://doi.org/10.30684/etj.v39i6.1593>

This is an open access article under the CC BY 4.0 license <http://creativecommons.org/licenses/by/4.0>

## 1. INTRODUCTION

Pulsed laser ablation in liquid has been established as a versatile technique to fabricate the manifold of colloidal nanoparticles [1] Thus far, this method has become increasingly beneficial along with its steady shift from fundamentals to applications [2]. Single nanoparticles (NPs) are of major interest because of their characteristic optical properties, catalytic activities and so on [3]. Nano-sized materials such as nanotubes, nanowires and NPs, display novel properties that vary from those of molecules and

bulk or individual atoms materials. Therefore, many research scientists aim to develop different methods for the synthesis of high-quality nanostructured materials. Amongst these nanoengineered materials, nickel oxide (NiO) with a wide bandgap (3.6–4 eV) [1,2] has attracted considerable interest as a strong candidate for many applications, such as solar cells, magnetic materials, gas sensors and catalysis. NiO NPs have been synthesized by various methods, such as spray pyrolysis, reverse-micellar route, sol-gel, microwave-assisted combustion, [4] and precipitation. PLA for the synthesis of nanostructured alloys and metal oxides in liquid media utilizing solid targets reported has been [5]. This method is a simple, high vacuum pumping system and does not require costly chambers. This technique's strategy for producing assorted nanomaterial is a direct, reliable, easy one-step approach that does not lack chemical precursors and scrimping agents, results in highly fresh and stable nanoparticles, its implemented at low temperature, awarded to further nanoscale manipulations and no need for any vacuum system [5].

Hence, it is considered a cleaner method. Research has shown that by changing various parameters, such as solution pH, laser wavelength, solution temperature and the addition of surfactants, one can control the size of synthesized materials and thereby alter their physical and chemical properties [6]. As a result of the different applications of NiO NPs, many methods for preparing NiO NPs have been applied. In particular, the PLA method has been reported to apply to the preparation of NiO NPs. Metal oxide semiconductors such as Cu<sub>2</sub>O [7], MnO<sub>2</sub> [8], CuO [9] and NiO [15] have been widely used for gas sensing. Amongst these sensing materials, NiO has attracted increasing attention as a highly useful sensing material for detecting oxidizing and reducing gases [10]. The aims of the present work is to study the influence of different laser fluences (1.27, 1.59, 1.9) J/cm<sup>2</sup> on optical, structural, surface morphology and the CO/CO<sub>2</sub> sensing properties. The three samples are presented which the first sample treated with 1.27J/cm<sup>2</sup> laser fluences, the second sample treated with 1.59J/cm<sup>2</sup> while the third sample treated with 1.9J/cm<sup>2</sup> laser fluence. This gives the chance to compare between the three samples in the properties that presented within this work.

## 2. EXPERIMENTAL PROCEDURE

Laser ablation was conducted on a piece of Ni fixed at the bottom of a glass container filled with 5 mL of liquid; ~3 mm of liquid was maintained over the top surface of the Ni block. Before the ablation process, Ni target was ultrasonically cleaned with acetone after cleaning with distilled water Figure.1 show Experimental setup of pulsed laser ablation. The Ni was immersed in distilled water and rotated by using a magnetic rotator to move the laser-irradiated position pulse by pulse. The Ni block was irradiated by an Nd:YAG Laser at 1064 nm. The pulse duration was 10 ns, and the repetition rate was 5 Hz. The lens showed a focal length of 250 mm, and the spot diameter of the laser beam on the nickel surface was usually 1 mm. The beaker was moved horizontally on the stage every minute to expose the fresh Ni surface of the beam. Pulse energies of 1.27, 1.59 and 1.9 J/cm<sup>2</sup> were used to observe the effects of pulse energy on the formation of Ni. The structure of the nickel oxide thin films was analyzed by (XRD) using an X-ray diffractometer (MiniFlex II, Rigaku, Japan). The wavelength of the X-ray source radiation (Cu, K $\alpha$ ) was 1.54 Å. Field emission scanning electron microscopy (FESEM) was performed using photoluminescence (PL, Hitachi-S4160, Japan) with a wavelength of 220–900 nm from Shimadzu, RF-5301 pc. From a gas test chamber made from a tube with a volume of 350 cm<sup>3</sup>, the gas delivery system has consisted. The chamber was provider through a connector that connected the gas sensor inside the chamber to the measuring equipment. On the opposite sides of the chamber, two valves were installed to serve as the gas inlet and outlet.

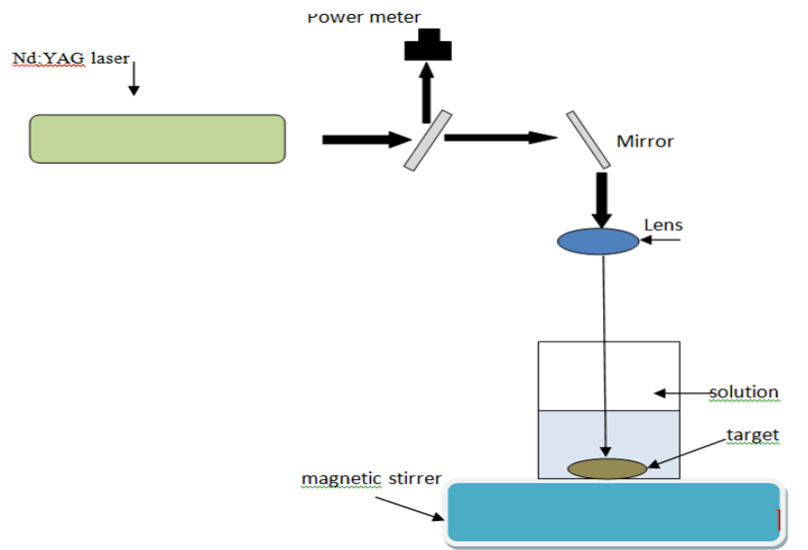


Figure 1: Experimental setup of pulsed laser ablation.

### 3. RESULT AND DISCUSSION

#### I. Structural Characteristics

The XRD patterns of the as-synthesized NiO films obtained using various laser fluences are shown in Figure (2). It was found that all the samples were polycrystalline. The existence of strong and sharp diffraction peaks at  $2\theta=37.26, 43.36, 62.86, 75.41$  and  $79.61$  corresponding to the (111), (200), (220), (311) and (222) crystal planes indicated the formation of a pure-phase cubic nickel oxide [11]. For the samples as-synthesized in different laser fluences, small peaks of nickel phase located at  $44.51, 51.81$  and  $76.31$  corresponding to fcc metallic Ni were observed. Figure (2) also shows the intensities of the (111), (200), (220) and (311) peaks that increased with increasing laser fluence. The average particle diameters (D) were calculated using the Debye-Scherrer formula and then listed in Equation 1.

$$D = 0.94 \times \lambda / \beta \cos \theta \quad (1)$$

where  $\lambda$  is the wavelength of the X-ray,  $\theta$  is the diffraction angle and  $\beta$  is the FWHM using different laser fluences ( $1.27, 1.59, 1.9$ )  $\text{J}/\text{cm}^2$ . Films undergo strain and dislocation in their structure, and these parameters were calculated [12] as Equations (2) and (3), respectively [13]. The calculated values are given in TABLE I

$$\varepsilon = \frac{\beta \cos \theta}{4} \quad (2)$$

$$\delta = \frac{1}{D^2} \quad (3)$$

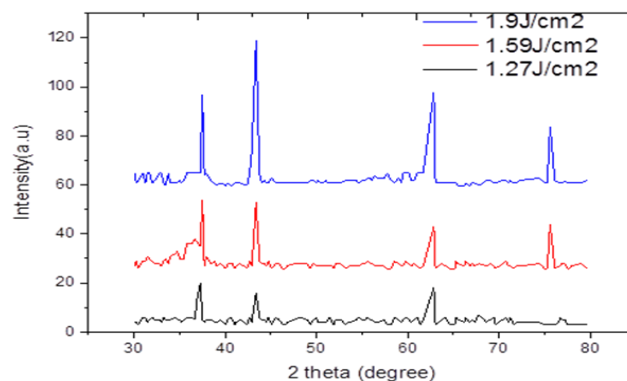


Figure 2: XRD pattern of as-synthesized NiO thin films

**TABLE I: Summary of X-Ray characterization.**

Floucnce(J/cm <sup>2</sup> )	Planes (hkl)	d(A°)	D (nm)	$\epsilon \times 10^{14}$ lines.m <sup>-2</sup>	$\delta$ strain $\times 10^{-4}$ lines <sup>-2</sup> . m <sup>-4</sup>
1.27	111	2.421	125.7	28	6.3
	200	2.063	26.55	13	14.2
	220	1.466	135.2	2.6	5.4
	311	1.261	131.6	2.7	5.77

## II. Field emission scanning electron microscopy FESEM Analysis

### Surface Morphology and Compositional Analysis

Figures 3(a)–(c) show the FESEM images of NiO for different laser fluences. The SEM images obviously show microstructural homogeneities and various morphologies for the as-synthesized NiO microparticles. The shapes of the as-synthesized NiO microparticles of the (1.27, 1.59, 1.9) J/cm<sup>2</sup> laser fluence-mediated samples are shown in Figures 3a–c. An agglomeration of NPs most has been observed in the instance, these images show snowflake-like morphologies, which consist of NiO microparticles that present spherical and elliptical shapes. The particles are almost spherical in shape. Our comparison of the images of NiO microparticles mentions that the particles produced in Figure 3c are much smaller than those produced in Figure 3(a, b). From the micrograph, we observed that grain sizes are not much uniform and that the average grain sizes of NiO thin films range from 298 nm to 526 nm. The average grain sizes determined by FESEM are comparatively greater than those measured by XRD; larger grain sizes may be due to the agglomeration of grains.

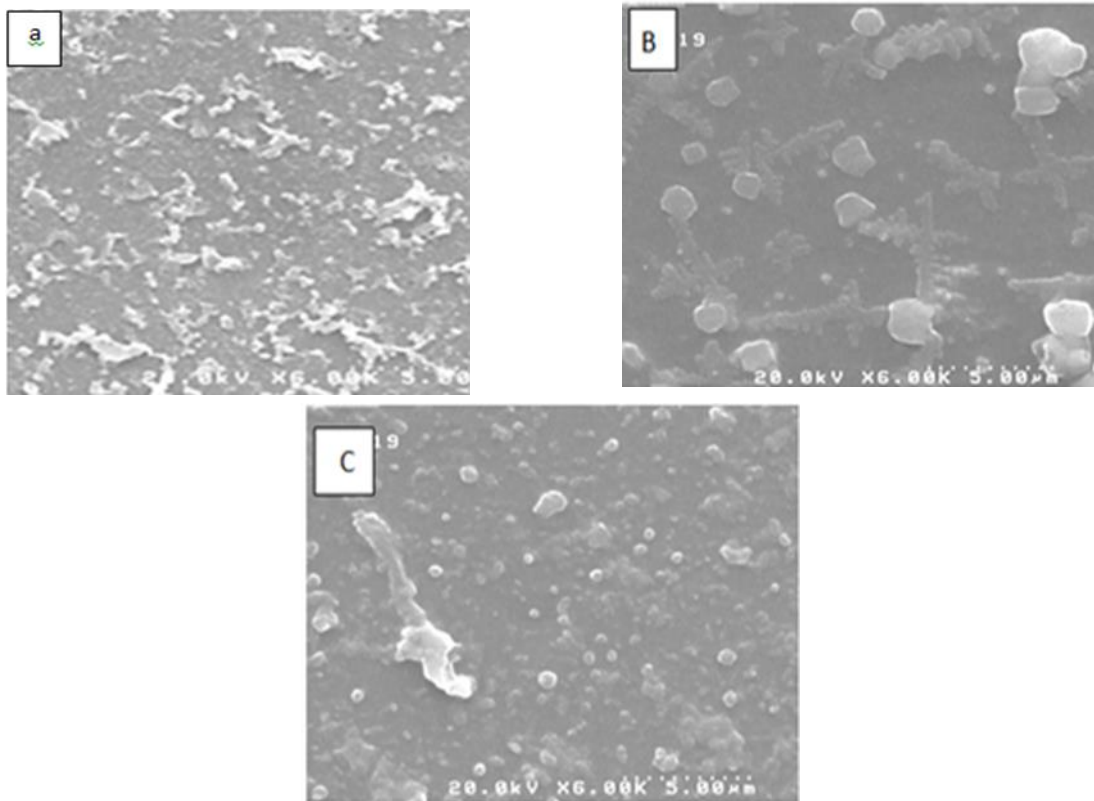


**Figure 3: (a. b. c) shows a FT SEM image of NiO microparticles**

### III. Photoluminescence results (PL)

Figure (4) illustrates the PL spectrum of the nickel oxide thin films prepared by the PLA at various laser fluences and excited at 325 nm. The PL spectra of the PLA-derived NiO thin films prepared at different laser fluencies contain different emission features, whose intensities and positions change with preparation conditions. Sample 1 shows two PL emission peaks. The near-band-edge emission band is in the range of 320-443 nm (broad emission), and the central value is 365 nm. The location of the UV emission centered at 365 nm does not change whilst the intensity strengthens as the laser fluence increases. A sharp peak noted as the second peak of sample 1 was localized at around 644 nm (narrow emission). In sample 2, the first peak centered at 310 nm, and the other peaks centered at 653 nm. The peak of sample 3 centered at 334 and 655 nm. The PL intensities of all peak positions of the UV missions for NiO thin films were clear and high. It indicated the direct transition of the electron band to band. This result suggested the crystalline structure of NiO. The emission of NiO (644,653,655) nm referred to film defects.

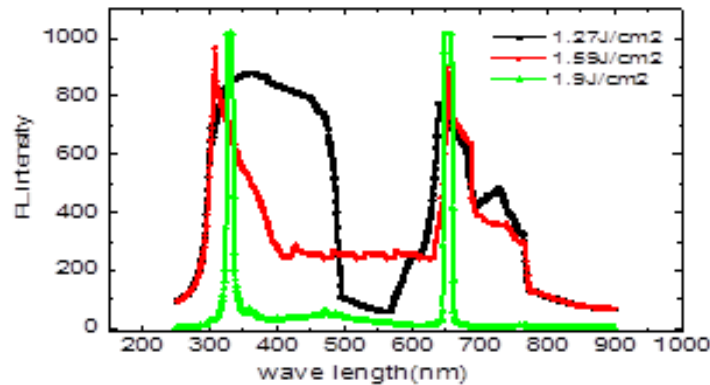


Figure 4: PL intensity of thin-film NiO for different laser fluence

### IV. Optical result

By using optical absorption (UV-Vis) and PL emission spectroscopies Optical properties were investigated. The photoabsorption spectra of the NiO thin films synthesized at different laser fluencies in double deionized water are shown in Figure (5). The absorption spectra clearly show a peak centered at around 360 nm and a tail extending to the red region (600 nm). The peak position shifts with increase laser fluence for various samples. The shift equates to low values in the visible and near-infrared regions. Following explained this result. High wavelength incident photons lack sufficient energy to interact with atoms. The photons undergo transmission when the wavelength reduces the interaction between incident photons and materials. In such a case, absorbance increases.

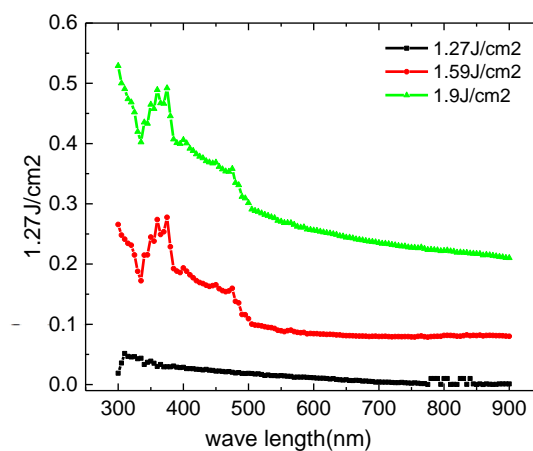


Figure 5: Absorbance of thin-film NiO for different laser fluence

### V. Gas sensing properties

The gas-sensing performance of the NiO was determined by measuring the different laser fluences on its films with different test gases (carbon monoxide, CO; carbon dioxide, CO<sub>2</sub>), as shown in Figure (6,7). The sensitivity of the NiO thin films to CO and CO<sub>2</sub> was studied. The gas sensitivity of the NiO films was calculated from the measured resistance variation in thin films in air and in CO and CO<sub>2</sub> gases. The variation in surface resistance in the presence of gas was measured by using Equation

$$= \text{Sensitivity} = (R_g - R_a) / R_a [14] \quad (4)$$

Figure (6.7) shows the film's sensitivity to different laser fluences. The figure also indicates that sensitivity increases with increasing operating time and reaches a saturation limit, from which it reverts to its original value within several minutes after stop gas exposure.

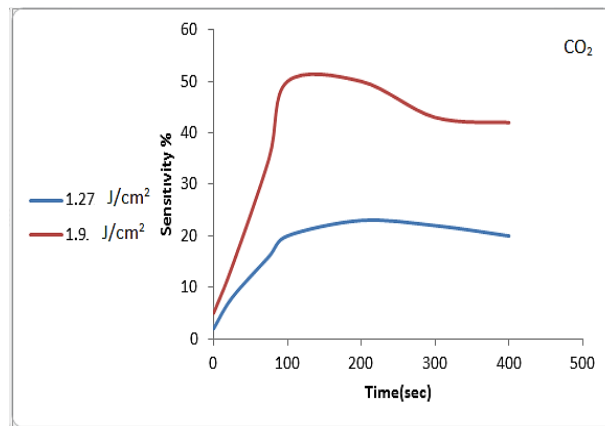


**Figure 6: Show the sensitivity of thin-film NiO for CO<sub>2</sub> gas for different laser fluence**

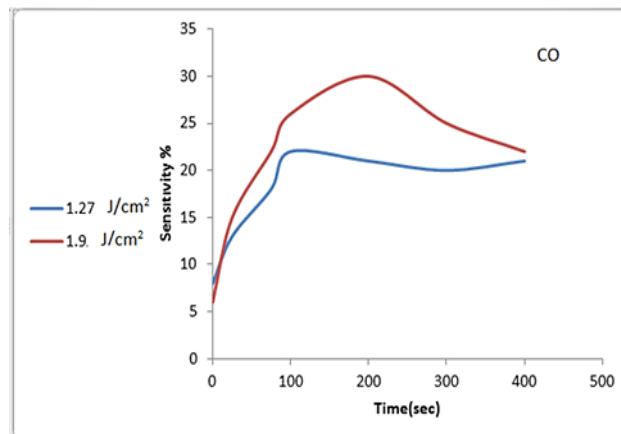


**Figure 7: Show the sensitivity of thin-film NiO for CO gas for different laser fluence**

Operating temperature is regarded as an important parameter for metal oxide semiconductors, and gas sensitivity is extremely dependent on it. Sensor sensitivity was investigated at different operating temperature, the results are shown in Figure (8,9). The sensitivity of the two sensors follows the same trend of increasing with temperature and then decreasing. The film's response to the fluence of 1.27 J/cm<sup>2</sup> is slow, whereas its response to a fluence of 1.9 J/cm<sup>2</sup> is rapid and presents an increase in sensitivity from 31% to 52%. Figures (8,9) show the film sensitivities for different laser fluences.

The mechanism of sensing oxidizing gas by NiO is elucidated as follows. When in contact with an oxidizing gas (electron acceptor), such as CO<sub>2</sub>, the negatively charged oxygen (O<sup>-</sup>) absorbed on the NiO film surface reacts. The reaction between the oxidizing gas and (O<sup>-</sup>) leads to an increase in sensitivity in the surface charge layer and a decrease in NiO resistance [15].

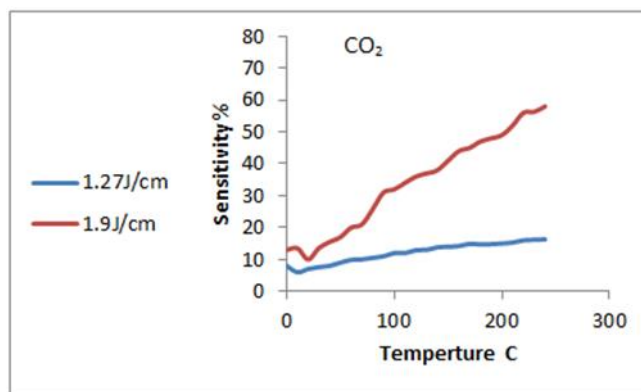


Figure 8: The sensitivity of thin-film NiO for CO<sub>2</sub> gas for different laser fluence

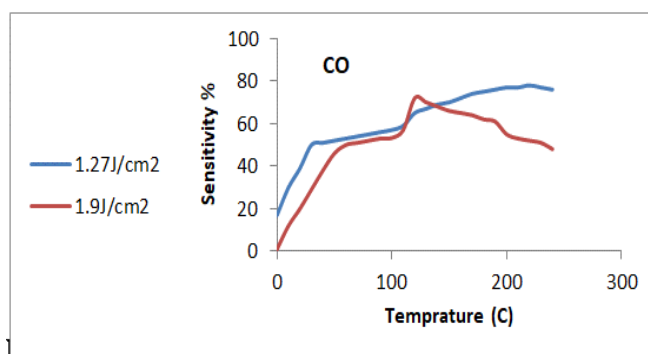


Figure 9: The sensitivity of thin-film NiO for CO gas for different laser fluence

#### 4. CONCLUSION

NiO microparticles have been successfully synthesized via laser ablation of high-purity Ni target in deionized water. To authority the properties of NiO particles, laser energy was a change from 0.27 to 1.9J/cm<sup>2</sup>. The prepared NiO microparticles were characterized by different techniques, including XRD, FESEM, UV-Vis and PL. All techniques showed significant changes in the structural, morphological and optical properties of the nickel oxide particles as laser fluence increases. The optical absorbance spectra of the samples showed the maximum value of around 360 nm. Scanning electron microscopy studies indicated that grain sizes are not much uniform and that the average grain sizes of NiO thin films range from 298 nm to 526 nm. Sensitivity and response time were improved by different laser fluences. The maximum sensitivity to CO gas is 80%. The sensors based on nickel oxide with great spherical particles showed superior gas sensing performance, including high gas response, relative to small spherical NiO particles.

#### REFERENCES

- [1] K. S. Khashan., G. M. Sulaiman., A. H. Hamed., Generation of NiO nanoparticles via pulsed laser ablation in deionized water and their antibacterial activity, *Appl. Phys. A*, 190 (2017). <https://doi.org/10.1007/s00339-017-0826-4>
- [2] S. Barcikowski, F. Mafune, Surface modification to Improve properties of materials, *J. Phys. Chem. C*, 115, (2011) 4985.
- [3] C. Indranath, B. Soumabha, L. Uzi, P. Thalappi, Atomically Precise Silver clusters as new SERS substrate, *J. Phys. Chem. Lett.*, 4 (2013) 2769-2773. <https://doi.org/10.1021/jz4014097>
- [4] J. P. Wilcoxon, J. E. Martin, F. Parsapour, B. Wiednman, D. F. Kelley, Photoluminescence from Nano size gold clusters, *J. Chem. Phys.*, 108 (1998). <https://doi.org/10.1063/1.476360>
- [5] M. Brust, M. Walker, D. Bethell, D. J. Schiffrin, R. Whyman, Gold nanorods Characterization for Nanomedical Applications, *J. Chem. Soc. Chem. Commun*, 7,801,1994.

- [6] M. Takesue, T. Tomura, M. Yamada, K. Hata, S. Kuwamoto, T. Yonezawa, Size of elementary cluster and process period in silver nanoparticle formation, *J. Am. Chem. Soc.*, 133 (2011) 14164-14167. <https://doi.org/10.1021/ja202815y>
- [7] M. Fumitaka, K. Jun-ya, T. Yoshihiro, K. Tamotsu, S. Hisahiro, Formation of gold nanoparticles by laser ablation in the aqueous solution of surfactant, *J. Phys. Chem. B*, 105 (2001) 5114-5120. <https://doi.org/10.1021/jp0037091>
- [8] L. Chenshitao, S. T. Navale, Z. B. Yang, Florian, Ethanol gas sensing properties of hydrothermally grown  $\alpha$ -MnO<sub>2</sub> nanorods, *J. Alloys Compd.*, 727 (2017) 362-369. <https://doi.org/10.1016/j.jallcom.2017.08.150>
- [9] L. Jiang, W. Zhang, A highly sensitive nonenzymatic glucose sensor based on CuO nanoparticles-modified carbon nanotube electrode, *Biosens. Bioelectron.*, 25 (2010) 1402-1407. <https://doi.org/10.1016/j.bios.2009.10.038>
- [10] C. Foukaraki, E. Bourithis, D. Tsamakis, A. Giannoudakos, M. Kompitsas, T. Xenidou, A. Boudouvis, Development of NiO-based thin films structures as efficient H<sub>2</sub> gas sensors operating at room temperatures, *Thin Solid Films*, 515 (2007) 8484-8489. <https://doi.org/10.1016/j.tsf.2007.03.147>
- [11] B. Sasi, K. Gopchandran, Nanostructured mesoporous nickel oxide thin films, *Nanotechnology*, 18 (2007). <https://doi.org/10.1088/0957-4484/18/11/115613>
- [12] P. S. Kireev, *Semiconductors physics*, Translated from Russian by M. Samokhvalov, MIR Publishers, Moscow (1978).
- [13] M. Liesegang, F. Tomaschek, Tracing the continental diagenetic loop of the opal-A to opal-CT transformation with X-ray diffraction, *Sediment. Geol.*, 398 (2020). <https://doi.org/10.1016/j.sedgeo.2020.105603>
- [14] F. Filippo, Surface interaction mechanisms in metal\_oxide semiconductors for alkane detection, *Universita Degli Studi di Ferrara, PHD*, 2008.
- [15] I. Hotovy, J. Huran, P. Siciliano, S. Capone, L. Spiess, V. Rehacek, Enhancement of H<sub>2</sub> sensing properties of NiO-based thin films with Pt surface modification, *Sens. Actuators B Chem.*, 103 (2004) 300-311. <https://doi.org/10.1016/j.snb.2004.04.109>